

Mode Switching for MIMO Broadcast Channel Based on Delay and Channel Quantization

Jun Zhang, Robert W. Heath Jr., Marios Kountouris, and Jeffrey G. Andrews

Abstract

Imperfect channel state information degrades the performance of multiple-input multiple-output (MIMO) communications; its effect on single-user (SU) and multi-user (MU) MIMO transmissions are quite different. In particular, MU-MIMO suffers from residual inter-user interference due to imperfect channel state information while SU-MIMO only suffers from a power loss. This paper compares the throughput loss of both SU and MU MIMO on the downlink due to delay and channel quantization. Accurate closed-form approximations are derived for the achievable rates for both SU and MU MIMO. It is shown that SU-MIMO is relatively robust to delayed and quantized channel information, while MU-MIMO with zero-forcing precoding loses spatial multiplexing gain with a fixed delay or fixed codebook size. Based on derived achievable rates, a mode switching algorithm is proposed that switches between SU and MU MIMO modes to improve the spectral efficiency, based on the average signal-to-noise ratio (SNR), the normalized Doppler frequency, and the channel quantization codebook size. The operating regions for SU and MU modes with different delays and codebook sizes are determined, which can be used to select the preferred mode. It is shown that the MU mode is active only when the normalized Doppler frequency is very small and the codebook size is large.

Index Terms

Multi-user MIMO, adaptive transmission, mode switching, imperfect channel state information at the transmitter (CSIT), zero-forcing precoding.

The authors are with the Wireless Networking and Communications Group, Department of Electrical and Computer Engineering, The University of Texas at Austin, 1 University Station C0803, Austin, TX 78712-0240. Email: {jzhang2, rheath, mkountouris, jandrews}@ece.utexas.edu. This work has been supported in part by AT&T Labs, Inc.

I. INTRODUCTION

Over the last decade, the point-to-point multiple-input multiple-output (MIMO) link (SU-MIMO) has been extensively researched and has transited from a theoretical concept to a practical technique [1], [2]. Due to space and complexity constraints, however, current mobile terminals only have one or two antennas, which limits the performance of the SU-MIMO link. Multi-user MIMO (MU-MIMO) provides the opportunity to overcome such a limitation by communicating with multiple mobiles simultaneously. It effectively increases the number of equivalent spatial channels and provides spatial multiplexing gain proportional to the number of transmit antennas at the base station even with single-antenna mobiles. In addition, MU-MIMO has higher immunity to propagation limitations faced by SU-MIMO, such as channel rank loss and antenna correlation [3].

There are many technical challenges that must be overcome to exploit the full benefits of MU-MIMO. A major one is the requirement of channel state information at the transmitter (CSIT), which is difficult to get especially for the downlink/broadcast channel. For the MIMO downlink with N_t transmit antennas and N_r receive antennas, with full CSIT the sum throughput can grow linearly with N_t even when $N_r = 1$, but without CSIT the spatial multiplexing gain is the same as for SU-MIMO, i.e. the throughput grows linearly with $\min(N_t, N_r)$ at high SNR [4]. Limited feedback is an efficient way to provide partial CSIT, which feeds back the quantized channel information to the transmitter via a low-rate feedback channel [5], [6]. However, such imperfect CSIT will greatly degrade the throughput gain provided by MU-MIMO [7], [8]. Besides quantization, there are other imperfections in the available CSIT, such as estimation error and feedback delay. With imperfect CSIT, it is not clear whether—or more to the point, when— MU-MIMO can outperform SU-MIMO. In this paper, we compare SU and MU-MIMO transmissions in the MIMO downlink with CSI delay and channel quantization, and propose to switch between SU and MU MIMO modes based on the achievable rate of each technique with practical receiver assumptions.

A. Related Work

For the MIMO downlink, CSIT is required to separate the spatial channels for different users. To obtain the full spatial multiplexing gain for the MU-MIMO system employing zero-forcing (ZF) or block-diagonalization (BD) precoding, it was shown in [7], [9] that the quantization

codebook size for limited feedback needs to increase linearly with SNR (in dB) and the number of transmit antennas. Zero-forcing dirty-paper coding and channel inversion systems with limited feedback were investigated in [8], where a sum rate ceiling due to a fixed codebook size was derived for both schemes. In [10], it was shown that to exploit multiuser diversity for ZF, both channel direction and information about signal-to-interference-plus-noise ratio (SINR) must be fed back. More recently, a comprehensive study of the MIMO downlink with ZF precoding was done in [11], which considered downlink training and explicit channel feedback and concluded that significant downlink throughput is achievable with efficient CSI feedback. For a compound MIMO broadcast channel, the information theoretic analysis in [12] showed that scaling the CSIT quality such that the CSIT error is dominated by the inverse of the SNR is both necessary and sufficient to achieve the full spatial multiplexing gain.

Although previous studies show that the spatial multiplexing gain of MU-MIMO can be achieved with limited feedback, it requires the codebook size to increase with SNR and the number of transmit antennas. Even if such a requirement is satisfied, there is an inevitable rate loss due to quantization error, plus other CSIT imperfections such as estimation error and delay. In addition, most of prior work focused on the achievable spatial multiplexing gain, mainly based on the analysis of the rate loss due to imperfect CSIT, which is usually a loose bound [7], [9], [12]. Such analysis cannot accurately characterize the throughput loss, and no comparison with SU-MIMO has been made. In this paper, we derive good approximations for the achievable throughput for both SU and MU MIMO systems with fixed channel information accuracy, i.e. with a fixed delay and a fixed quantization codebook size. We are interested in the following question: *With imperfect CSIT, including delay and channel quantization, when can MU-MIMO actually deliver a throughput gain over SU-MIMO?* Based on this, we can select the one with the higher throughput as the transmission technique.

B. Contributions

In this paper, we investigate SU and MU-MIMO in the broadcast channel with CSI delay and limited feedback. The main contributions of this paper are as follows.

- **SU vs. MU Analysis.** We investigate the impact of imperfect CSIT due to delay and channel quantization. We show that the SU mode is more robust to imperfect CSIT as it only suffers a constant rate loss, while MU-MIMO suffers more severely from the residual inter-user

interference. We characterize the residual interference due to delay and channel quantization, which shows these two effects are equivalent. Based on an independence approximation of the interference terms and the signal term, accurate closed-form approximations are derived for the ergodic rates for both SU and MU MIMO modes.

- **Mode Switching Algorithm.** A SU/MU mode switching algorithm is proposed based on the ergodic sum rate as a function of the average SNR, normalized Doppler frequency, and the quantization codebook size. This transmission technique only requires a small number of users to feed back instantaneous channel information. The mode switching points can be calculated from the previously derived approximations for ergodic rates.
- **Operating Regions.** The *operating regions* for SU and MU modes are determined, from which we can determine the active mode and find the condition that activates each mode. With a fixed delay and codebook size, if the MU mode is possible at all, there are two mode switching points, with the SU mode preferred at both low and high SNRs. The MU mode will only be activated when the normalized Doppler frequency is very small and the codebook size is large. From the numerical results, the minimum feedback bits per user to get the MU mode activated grow approximately linearly with the number of transmit antennas.

The rest of the paper is organized as follows. The system model and some assumptions are presented in Section II. The transmission techniques for both SU and MU MIMO modes are described in Section III. The rate analysis for both SU and MU modes and the mode switching are done in Section IV. Numerical results and conclusions are in Section V and VI, respectively.

II. SYSTEM MODEL

We consider a MIMO downlink, where the transmitter (the base station) has N_t antennas and each mobile user has a single antenna. The system parameters are listed in Table I. During each transmission period, which is less than the channel coherence time and the channel is assumed to be constant, the base station transmits to one (SU-MIMO mode) or multiple (MU-MIMO mode) users. The discrete-time complex baseband received signal at the u -th user at time n is

given as¹

$$y_u[n] = \mathbf{h}_u^*[n] \sum_{u'=1}^U \mathbf{f}_{u'}[n] x_{u'}[n] + z_u[n], \quad (1)$$

where $\mathbf{h}_u[n]$ is the $N_t \times 1$ channel vector from the transmitter to the u -th user, and $z_u[n]$ is the normalized complex Gaussian noise vector, i.e. $z_u[n] \sim \mathcal{CN}(0, 1)$. $x_u[n]$ and $\mathbf{f}_u[n]$ are the transmit signal and $N_t \times 1$ precoding vector for the u -th user, respectively. The transmit power constraint is $\mathbb{E}\{\mathbf{x}^*[n]\mathbf{x}[n]\} = P$, where $\mathbf{x}[n] = [x_1^*, x_2^*, \dots, x_U^*]^*$. As the noise is normalized, P is also the average transmit SNR.

To assist the analysis, we assume that the channel $\mathbf{h}_u[n]$ is well modeled as a spatially white Gaussian channel, with entries $h_{i,j}[n] \sim \mathcal{CN}(0, 1)$, and the channels are i.i.d. over different users. The results will be different for different channel models. For example, a limited feedback system with line of sight MIMO channel requires fewer feedback bits compared to the Rayleigh channel [13]. The investigation of other channel models is left to future work.

We consider two of the main sources of the CSIT imperfection—delay and quantization error², specified as follows.

A. CSI Delay Model

We consider a stationary ergodic Gauss-Markov block fading process [14, Sec. 16–1], where the channel stays constant for a symbol duration and changes from symbol to symbol according to

$$\mathbf{h}[n] = \rho \mathbf{h}[n-1] + \mathbf{e}[n], \quad (2)$$

where $\mathbf{e}[n]$ is the channel error vector, with i.i.d. entries $e_i[n] \sim \mathcal{CN}(0, \epsilon_e^2)$, and it is uncorrelated with $\mathbf{h}[n-1]$. We assume the CSI delay is of one symbol. It is straightforward to extend the results to the scenario with a delay of multiple symbols. For the numerical analysis, the classical Clarke's isotropic scattering model will be used as an example, for which the correlation coefficient is

¹In this paper, we use uppercase boldface letters for matrices (\mathbf{X}) and lowercase boldface for vectors (\mathbf{x}). $\mathbb{E}[\cdot]$ is the expectation operator. The conjugate transpose of a matrix \mathbf{X} (vector \mathbf{x}) is \mathbf{X}^* (\mathbf{x}^*). Similarly, \mathbf{X}^\dagger denotes the pseudo-inverse, $\tilde{\mathbf{x}}$ denotes the normalized vector of \mathbf{x} , i.e. $\tilde{\mathbf{x}} = \frac{\mathbf{x}}{\|\mathbf{x}\|}$, and $\hat{\mathbf{x}}$ denotes the quantized vector of $\tilde{\mathbf{x}}$.

²For a practical system, the feedback bits for each user is usually fixed, and there will inevitably be delay in the available CSI, both of which are difficult or even impossible to adjust. Other effects such as channel estimation error can be made small such as by increasing the transmit power or the number of pilot symbols.

$\rho = J_0(2\pi f_d T_s)$ with Doppler spread f_d [15], where $J_0(\cdot)$ is the zero-th order Bessel function of the first kind. The variance of the error vector is $\epsilon_e^2 = 1 - \rho^2$. Therefore, both ρ and ϵ_e are determined by the normalized Doppler frequency $f_d T_s$.

The channel in (2) is widely-used to model the time-varying channel. For example, it is used to investigate the impact of feedback delay on the performance of closed-loop transmit diversity in [16] and the system capacity and bit error rate of point-to-point MIMO link in [17]. It simplifies the analysis, and the results can be easily extended to other scenarios. Essentially, this model is of the form

$$\mathbf{h}[n] = \mathbf{g}[n] + \mathbf{e}[n], \quad (3)$$

where $\mathbf{g}[n]$ is the available CSI at time n with an uncorrelated error vector $\mathbf{e}[n]$, $\mathbf{g}[n] \sim \mathcal{CN}(\mathbf{0}, (1 - \epsilon_e^2)\mathbf{I})$, and $\mathbf{e}[n] \sim \mathcal{CN}(\mathbf{0}, \epsilon_e^2\mathbf{I})$. It can be used to consider the effect of other imperfect CSIT, such as estimation error and analog feedback. The difference is in $\mathbf{e}[n]$, which has different variance ϵ_e^2 for different scenarios. Some examples are given as follows.

a) Estimation Error: If the receiver obtains the CSI through MMSE estimation from τ_p pilot symbols, the error variance is $\epsilon_e^2 = \frac{1}{1 + \tau_p \gamma_p}$, where γ_p is the SNR of the pilot symbol [18].

b) Analog Feedback: For analog feedback, the error variance is $\epsilon_e^2 = \frac{1}{1 + \tau_{ul} \gamma_{ul}}$, where τ_{ul} is the number of channel uses per channel coefficient and γ_{ul} is the SNR on the uplink feedback channel [19].

c) Analog Feedback with Prediction: As shown in [20], for analog feedback with a d -step MMSE predictor and the Gauss-Markov model, the error variance is $\epsilon_e^2 = \rho^{2d} \epsilon_0 + (1 - \rho^2) \sum_{l=0}^{d-1} \rho^{2l}$, where ρ is the same as in (2) and ϵ_0 is the Kalman filtering mean-square error.

Therefore, the results in this paper can be easily extended to these systems. In the following parts, we focus on the effect of CSI delay.

B. Channel Quantization Model

We consider frequency-division duplexing (FDD) systems, where limited feedback techniques provide partial CSIT through a dedicated feedback channel from the receiver to the transmitter. The channel direction information for the precoder design is fed back using a quantization codebook known at both the transmitter and receiver.

The quantization is chosen from a codebook of unit norm vectors of size $L = 2^B$. We assume each user uses a different codebook to avoid the same quantization vector. The codebook for

user u is $\mathcal{C}_u = \{\mathbf{c}_{u,1}, \mathbf{c}_{u,2}, \dots, \mathbf{c}_{u,L}\}$. Each user quantizes its channel to the closest codeword, where closeness is measured by the inner product. Therefore, the index of channel for user u is

$$I_u = \arg \max_{1 \leq \ell \leq L} |\tilde{\mathbf{h}}_u^* \mathbf{c}_{u,\ell}|. \quad (4)$$

Each user needs to feed back B bits to denote this index, and the transmitter has the quantized channel information $\hat{\mathbf{h}}_u = \mathbf{c}_{u,I_u}$. As the optimal vector quantizer for this problem is not known in general, random vector quantization (RVQ) [21] is used, where each quantization vector is independently chosen from the isotropic distribution on the N_t -dimensional unit sphere. It has been shown in [7] that RVQ can facilitate the analysis and provide performance close to the optimal quantization. In this paper, we analyze the achievable rate averaged over both RVQ-based random codebooks and fading distributions.

An important metric for the limited feedback system is the squared angular distortion, defined as $\sin^2(\theta_u) = 1 - |\tilde{\mathbf{h}}_u^* \hat{\mathbf{h}}_u|^2$, where $\theta_u = \angle(\tilde{\mathbf{h}}_u, \hat{\mathbf{h}}_u)$. With RVQ, it was shown in [7], [22] that the expectation in i.i.d. Rayleigh fading is given by

$$\mathbb{E}_\theta [\sin^2(\theta_u)] = 2^B \cdot \beta\left(2^B, \frac{N_t}{N_t - 1}\right), \quad (5)$$

where $\beta(\cdot)$ is the beta function. It can be tightly bounded as [7]

$$\frac{N_t - 1}{N_t} 2^{-\frac{B}{N_t - 1}} \leq \mathbb{E} [\sin^2(\theta_u)] \leq 2^{-\frac{B}{N_t - 1}}. \quad (6)$$

III. TRANSMISSION TECHNIQUES

In this section, we describe the transmission techniques for both SU and MU MIMO systems with perfect CSIT, which will be used in the subsequent sections for imperfect CSIT systems. By doing this, we focus on the impacts of imperfect CSIT on the conventional transmission techniques. Designing imperfect CSIT-aware precoders is left to future work. Throughout this paper, we use the achievable ergodic rate as the performance metric for both SU and MU-MIMO systems. The base station transmits to a single user ($U = 1$) for the SU-MIMO system and to N_t users ($U = N_t$) for the MU-MIMO system. The SU/MU mode switching algorithm is also described.

A. SU-MIMO System

With perfect CSIT, it is optimal for the SU-MIMO system to transmit along the channel direction [1], i.e. selecting the beamforming (BF) vector as $\mathbf{f}[n] = \tilde{\mathbf{h}}[n]$, denoted as *eigen-beamforming* in this paper. The ergodic capacity of this system is the same as that of a maximal ratio combining diversity system, given by [23]

$$R_{BF}(P) = \mathbb{E}_{\mathbf{h}} [\log_2 (1 + P \|\mathbf{h}[n]\|^2)] = \log_2(e) e^{1/P} \sum_{k=0}^{N_t-1} \frac{\Gamma(-k, 1/P)}{P^k}, \quad (7)$$

where $\Gamma(\cdot, \cdot)$ is the complementary incomplete gamma function defined as $\Gamma(\alpha, x) = \int_x^\infty t^{\alpha-1} e^{-t} dt$.

B. MU-MIMO System

For MIMO broadcast channels, although dirty-paper coding (DPC) [24] is optimal [25]–[29], it is difficult to implement in practice. As in [7], [11], ZF precoding is used in this paper, which is a linear precoding technique that precancels inter-user interference at the transmitter. There are several reasons for us to use this simple transmission technique. Firstly, due to its simple structure, it is possible to derive closed-form results, which can provide helpful insights. Second, the ZF precoding is able to provide full spatial multiplexing gain and only has a power offset compared to the optimal DPC system [30]. In addition, it was shown in [30] that the ZF precoding is optimal among the set of all linear precoders at asymptotically high SNR. In Section V, we will show that our results for the ZF system also apply for the regularized ZF precoding [31], which provides a higher throughput than the ZF precoding at low to moderate SNRs.

With precoding vectors $\mathbf{f}_u[n]$, $u = 1, 2, \dots, U$, assuming equal power allocation³, the received SINR for the u -th user is given as

$$\gamma_{ZF,u} = \frac{\frac{P}{U} |\mathbf{h}_u^*[n] \mathbf{f}_u[n]|^2}{1 + \frac{P}{U} \sum_{u' \neq u} |\mathbf{h}_u^*[n] \mathbf{f}_{u'}[n]|^2}.$$

This is true for a general linear precoding MU-MIMO system. With perfect CSIT, this quantity can be calculated at the transmitter, while with imperfect CSIT, it can be estimated at the receiver and fed back to the transmitter given knowledge of $\mathbf{f}_u[n]$.

³At high SNR, this performs closely to the system employing optimal water-filling, as power allocation mainly benefits at low SNR.

Denote $\tilde{\mathbf{H}}[n] = [\tilde{\mathbf{h}}_1[n], \tilde{\mathbf{h}}_2[n], \dots, \tilde{\mathbf{h}}_U[n]]^*$. With perfect CSIT, the ZF precoding vectors are determined from the pseudo-inverse of $\tilde{\mathbf{H}}[n]$, as $\mathbf{F}[n] = \tilde{\mathbf{H}}^\dagger[n] = \tilde{\mathbf{H}}^*[n](\tilde{\mathbf{H}}[n]\tilde{\mathbf{H}}^*[n])^{-1}$. The precoding vector for the u -th user is obtained by normalizing the u -th column of $\mathbf{F}[n]$. Therefore, $\mathbf{h}_u^*[n]\mathbf{f}_{u'}[n] = 0, \forall u \neq u'$, i.e. there is no inter-user interference. The received SINR for the u -th user becomes

$$\gamma_{ZF,u} = \frac{P}{U} |\mathbf{h}_u^*[n]\mathbf{f}_u[n]|^2. \quad (8)$$

As $\mathbf{f}_u[n]$ is independent of $\mathbf{h}_u[n]$, and $\|\mathbf{f}_u[n]\|^2 = 1$, the effective channel for the u -th user is a single-input single-output (SISO) Rayleigh fading channel. Therefore, the achievable sum rate for the ZF system is given by

$$R_{ZF}(P) = \sum_{u=1}^U \mathbb{E}_\gamma [\log_2(1 + \gamma_{ZF,u})]. \quad (9)$$

Each term on the right hand side of (9) is the ergodic capacity of a SISO system in Rayleigh fading, given in [23] as

$$R_{ZF,u} = \mathbb{E}_\gamma [\log_2(1 + \gamma_{ZF,u})] = \log_2(e) e^{U/P} E_1(U/P), \quad (10)$$

where $E_1(\cdot)$ is the exponential-integral function of the first order, $E_1(x) = \int_1^\infty \frac{e^{-xt}}{t} dt$.

C. SU/MU Mode Switching

Imperfect CSIT will degrade the performance of the MIMO communication. In this case, it is unclear whether and when the MU-MIMO system can actually provide a throughput gain over the SU-MIMO system. Based on the analysis of the achievable ergodic rates in this paper, we propose to switch between SU and MU modes and select the one with the higher achievable rate.

The channel correlation coefficient ρ , which captures the CSI delay effect, usually varies slowly. The quantization codebook size is normally fixed for a given system. Therefore, it is reasonable to assume that the transmitter has knowledge of both delay and channel quantization, and can estimate the achievable ergodic rates of both SU and MU MIMO modes. Then it can determine the active mode and select one (SU mode) or N_t (MU mode) users to serve. This is a low-complexity transmission strategy, and can be combined with random user selection, round-robin scheduling, or scheduling based on queue length rather than channel status. It only requires the selected users to feed back instantaneous channel information. Therefore, it is suitable for a

system that has a constraint on the total feedback bits and only allows a small number of users to send feedback, or a system with a strict delay constraint that cannot employ opportunistic scheduling based on instantaneous channel information.

To determine the transmission rate, the transmitter sends pilot symbols, from which the active users estimate the received SINRs and feed back them to the transmitter. In this paper, we assume the transmitter knows perfectly the actual received SINR at each active user. In practice, there will inevitably be errors in such information due to estimation error and feedback delay, which will result in rate mismatch, i.e. the transmission rate based on the estimated SINR does not match the actual SINR on the channel, so there will be outage events. How to deal with such rate mismatch is of practical importance, and we mention several possible approaches as follows. The full investigation of this issue requires further research and is out of scope of this paper. Considering the outage events, the transmission strategy can be designed based on the actual information symbols successfully delivered to the receiver, denoted as *goodput* in [32], [33]. With the estimated SINR, another approach is to back off on the transmission rate based on the variance of the estimation error, as did in [34], [35] for the single-antenna opportunistic scheduling system and in [36] for the multiple-antenna opportunistic beamforming system. Combined with user selection, the transmission rate can also be determined based on some lower bound of the actual SINR to make sure that no outage occurs, as did in [37] for the limited feedback system.

IV. PERFORMANCE ANALYSIS AND MODE SWITCHING

In this section, we investigate the achievable ergodic rates for both SU and MU MIMO modes. We first analyze the average received SNR for the BF system and the average residual interference for the ZF system, which provide insights on the impact of imperfect CSIT. To select the active mode, accurate closed-form approximations for both SU and MU modes are then derived.

A. SU Mode–Eigen-Beamforming

First, if there is no delay and only channel quantization, the BF vector is based on the quantized feedback, $\mathbf{f}^{(Q)}[n] = \hat{\mathbf{h}}[n]$. The average received SNR is

$$\overline{\text{SNR}}_{BF}^{(Q)} = \mathbb{E}_{\mathbf{h},c}[P|\mathbf{h}^*[n]\hat{\mathbf{h}}[n]|^2]$$

$$\begin{aligned}
&= \mathbb{E}_{\mathbf{h}, \mathcal{C}}[P \|\mathbf{h}[n]\|^2 |\tilde{\mathbf{h}}^*[n] \hat{\mathbf{h}}[n]|^2] \\
&\stackrel{(a)}{\leq} P N_t \left(1 - \frac{N_t - 1}{N_t} 2^{-\frac{B}{N_t - 1}} \right), \tag{11}
\end{aligned}$$

where (a) follows the independence between $\|\mathbf{h}[n]\|^2$ and $|\tilde{\mathbf{h}}^*[n] \hat{\mathbf{h}}[n]|^2$, together with the result in (6).

With both delay and channel quantization, the BF vector is based on the quantized channel direction with delay, i.e. $\mathbf{f}^{(QD)}[n] = \hat{\mathbf{h}}[n-1]$. The instantaneous received SNR for the BF system

$$\text{SNR}_{BF}^{(QD)} = P \left| \mathbf{h}^*[n] \mathbf{f}^{(QD)}[n] \right|^2. \tag{12}$$

Based on (11), we get the following theorem on the average received SNR for the SU mode.

Theorem 1: The average received SNR for a BF system with channel quantization and CSI delay is

$$\overline{\text{SNR}}_{BF}^{(QD)} \leq P N_t \left(\rho^2 \Delta_{BF}^{(Q)} + \Delta_{BF}^{(D)} \right), \tag{13}$$

where $\Delta_{BF}^{(Q)}$ and $\Delta_{BF}^{(D)}$ show the impact of channel quantization and feedback delay, respectively, given by

$$\Delta_{BF}^{(Q)} = 1 - \frac{N_t - 1}{N_t} 2^{-\frac{B}{N_t - 1}}, \quad \Delta_{BF}^{(D)} = \frac{\epsilon_e^2}{N_t}.$$

Proof: See Appendix B. ■

From Jensen's inequality, an upper bound of the achievable rate for the BF system with both quantization and delay is given by

$$\begin{aligned}
R_{BF}^{(QD)} &= \mathbb{E}_{\mathbf{h}, \mathcal{C}} \left[\log_2 \left(1 + \text{SNR}_{BF}^{(QD)} \right) \right] \\
&\leq \log_2 \left[1 + \overline{\text{SNR}}_{BF}^{(QD)} \right] \\
&\leq \log_2 \left[1 + P N_t \left(\rho^2 \Delta_{BF}^{(Q)} + \Delta_{BF}^{(D)} \right) \right]. \tag{14}
\end{aligned}$$

Remark 1: Note that $\rho^2 = 1 - \epsilon_e^2$, so the average SNR decreases with ϵ_e^2 . With a fixed B and fixed delay, the SNR degradation is a constant factor independent of P . At high SNR, the imperfect CSIT introduces a constant rate loss $\log_2 \left(\rho^2 \Delta_{BF}^{(Q)} + \Delta_{BF}^{(D)} \right)$.

The upper bound provided by Jensen's inequality is not tight. To get a better approximation for the achievable rate, we first make the following approximation on the instantaneous received

SNR

$$\begin{aligned}
\text{SNR}_{BF}^{(QD)} &= P|\mathbf{h}^*[n]\hat{\mathbf{h}}[n-1]|^2 \\
&= P|(\rho\mathbf{h}[n-1] + \mathbf{e}[n])^*\hat{\mathbf{h}}[n-1]|^2 \\
&\approx P\rho^2|\mathbf{h}^*[n-1]\hat{\mathbf{h}}[n-1]|^2,
\end{aligned} \tag{15}$$

i.e. we remove the term with $\mathbf{e}[n]$ as it is normally insignificant compared to $\rho\mathbf{h}[n-1]$. This will be verified later by simulation. In this way, the system is approximated as the one with limited feedback and with equivalent SNR $\rho^2 P$.

From [22], the achievable rate of the limited feedback BF system is given by

$$\begin{aligned}
R_{BF}^{(Q)}(P) &= \log_2(e) \left(e^{1/P} \sum_{k=0}^{N_t-1} E_{k+1} \left(\frac{1}{P} \right) \right. \\
&\quad \left. - \int_0^1 (1 - (1-x)^{N_t-1})^{2^B} \frac{N_t}{x} e^{1/Px} E_{N_t+1} \left(\frac{1}{Px} \right) dx \right),
\end{aligned} \tag{16}$$

where $E_n(x) = \int_1^\infty e^{-xt} x^{-n} dt$ is the n -th order exponential integral. So $R_{BF}^{(QD)}$ can be approximated as

$$R_{BF}^{(QD)}(P) \approx R_{BF}^{(Q)}(\rho^2 P). \tag{17}$$

As a special case, considering a system with delay only, e.g. the time-division duplexing (TDD) system which can estimate the CSI from the uplink with channel reciprocity but with propagation and processing delay, the BF vector is based on the delayed channel direction, i.e. $\mathbf{f}^{(D)}[n] = \tilde{\mathbf{h}}[n-1]$. We provide a good approximation for the achievable rate for such a system as follows.

The instantaneous received SNR is given as

$$\begin{aligned}
\text{SNR}_{BF}^{(D)} &= P|\mathbf{h}^*[n]\mathbf{f}^{(D)}[n]|^2 \\
&= P|(\rho\mathbf{h}[n-1] + \mathbf{e}[n])^*\tilde{\mathbf{h}}[n-1]|^2 \\
&\stackrel{(a)}{\approx} P\rho^2\|\mathbf{h}[n-1]\|^2 + P|\mathbf{e}^*[n]\tilde{\mathbf{h}}[n-1]|^2.
\end{aligned} \tag{18}$$

In step (a) we eliminate the cross terms since $\mathbf{e}[n]$ is normally small. As $\mathbf{e}[n]$ is independent of $\tilde{\mathbf{h}}[n-1]$, $\mathbf{e}[n] \sim \mathcal{CN}(\mathbf{0}, \epsilon_e^2 \mathbf{I})$ and $\|\tilde{\mathbf{h}}[n-1]\|^2 = 1$, we have $|\mathbf{e}^*[n]\tilde{\mathbf{h}}[n-1]|^2 \sim \chi_2^2$, where χ_M^2 denotes chi-square distribution with M degrees of freedom. In addition, $\|\mathbf{h}[n-1]\|^2 \sim \chi_{2N_t}^2$, and it is independent of $|\mathbf{e}^*[n]\tilde{\mathbf{h}}[n-1]|^2$. Then the following theorem can be derived.

Theorem 2: The achievable ergodic rate of the BF system with delay can be approximated as

$$R_{BF}^{(D)} \approx \log_2(e) a_0^{N_t} e^{1/\eta_2} E_1\left(\frac{1}{\eta_2}\right) - \log_2(e) (1 - a_0) \sum_{i=0}^{N_t-1} \sum_{l=0}^i \frac{a_0^{N_t-1-i}}{(i-l)!} \eta_1^{-(i-l)} I_1(1/\eta_1, 1, i-l), \quad (19)$$

where $\eta_1 = P\rho^2$, $\eta_2 = P\epsilon_e^2$, $a_0 = \frac{\eta_2}{\eta_2 - \eta_1}$, and $I_1(\cdot, \cdot, \cdot)$ is given in (36) in Appendix A.

Proof: See Appendix C. ■

B. Zero-Forcing

1) *Average Residual Interference:* If there is no delay and only channel quantization, the precoding vectors for the ZF system are designed based on $\hat{\mathbf{h}}_1[n], \hat{\mathbf{h}}_2[n], \dots, \hat{\mathbf{h}}_U[n]$ to achieve $\hat{\mathbf{h}}_u^*[n] \mathbf{f}_{u'}^{(Q)}[n] = 0, \forall u \neq u'$. With random vector quantization, it is shown in [7] that the average noise plus interference for each user is

$$\Delta_{ZF,u}^{(Q)} = \mathbb{E}_{\mathbf{h}, \mathcal{C}} \left[1 + \frac{P}{U} \sum_{u' \neq u} |\mathbf{h}_u^*[n] \mathbf{f}_{u'}^{(Q)}[n]|^2 \right] = 1 + 2^{-\frac{B}{N_t-1}} P. \quad (20)$$

With both channel quantization and CSI delay, precoding vectors are designed based on $\hat{\mathbf{h}}_1[n-1], \hat{\mathbf{h}}_2[n-1], \dots, \hat{\mathbf{h}}_U[n-1]$ and achieve $\hat{\mathbf{h}}_u^*[n-1] \mathbf{f}_{u'}^{(QD)}[n] = 0, \forall u \neq u'$. The received SINR for the u -th user is given as

$$\gamma_{ZF,u}^{(QD)} = \frac{\frac{P}{U} |\mathbf{h}_u^*[n] \mathbf{f}_u^{(QD)}[n]|^2}{1 + \frac{P}{U} \sum_{u' \neq u} |\mathbf{h}_u^*[n] \mathbf{f}_{u'}^{(QD)}[n]|^2}. \quad (21)$$

As $\mathbf{f}_u^{(QD)}[n]$ is in the nullspace of $\hat{\mathbf{h}}_{u'}[n-1] \forall u' \neq u$, it is isotropically distributed in \mathbb{C}^{N_t} and independent of $\tilde{\mathbf{h}}_u[n-1]$ as well as $\tilde{\mathbf{h}}_u[n]$, so $|\mathbf{h}_u^*[n] \mathbf{f}_u^{(QD)}[n]|^2 \sim \chi_2^2$. The average noise plus interference is given in the following theorem.

Theorem 3: The average noise plus interference for the u -th user of the ZF system with both channel quantization and CSI delay is

$$\Delta_{ZF,u}^{(QD)} = 1 + (U-1) \frac{P}{U} \left(\rho_u^2 \Delta_{ZF,u}^{(Q)} + \Delta_{ZF,u}^{(D)} \right), \quad (22)$$

where $\Delta_{ZF,u}^{(Q)}$ and $\Delta_{ZF,u}^{(D)}$ are the degradations brought by channel quantization and feedback delay, respectively, given by

$$\Delta_{ZF,u}^{(Q)} = \frac{U}{U-1} 2^{-\frac{B}{N_t-1}}, \quad \Delta_{ZF,u}^{(D)} = \epsilon_{e,u}^2.$$

Proof: The proof is similar to the one for *Theorem 1* in appendix B. ■

Remark 2: From *Theorem 3* we see that the average residual interference for a given user consists of three parts:

- (i) *The number of interferers, $U - 1$.* The more users the system supports, the higher the mutual interference.
- (ii) *The transmit power of the other active users, $\frac{P}{U}$.* As the transmit power increases, the system becomes interference-limited. It is possible to improve performance through power allocation, which is left to future work.
- (iii) *The CSIT accuracy for this user,* which is reflected from $\rho_u^2 \Delta_{ZF,u}^{(Q)} + \Delta_{ZF,u}^{(D)}$. The user with a larger delay or a smaller codebook size suffers a higher residual interference.

From this remark, the interference term, $\frac{P}{U}(U - 1)\epsilon_{e,u}^2$, equivalently comes from $U - 1$ *virtual interfering users*, each with equivalent SNR as $\frac{P}{U} \left(\rho_u^2 \Delta_{ZF,u}^{(Q)} + \Delta_{ZF,u}^{(D)} \right)$. With a high P and a fixed $\epsilon_{e,u}$ or B , the system is interference-limited and cannot achieve full spatial multiplexing gain. Therefore, to keep a constant rate loss, i.e. to sustain the spatial multiplexing gain, the channel error due to both quantization and delay needs to be reduced as SNR increases. Similar to the result for the limited feedback system in [7], for the ZF system with both delay and channel quantization, we can get the following corollary for the condition to achieve the full spatial multiplexing gain.

Corollary 1: To keep a constant rate loss of $\log_2 \delta_0$ bps/Hz for each user, the codebook size and CSI delay need to satisfy the following condition

$$\rho_u^2 \Delta_{ZF,u}^{(Q)} + \Delta_{ZF,u}^{(D)} = \frac{U}{U - 1} \cdot \frac{\delta_0 - 1}{P}. \quad (23)$$

Proof: As shown in [7], [11], the rate loss for each user due to imperfect CSIT is upper bounded by $\Delta R_u \leq \log_2 \Delta_{ZF,u}^{(QD)}$. The corollary follows from solving $\log_2 \Delta_{ZF,u}^{(QD)} = \log_2 \delta_0$. ■

Equivalently, this means that for a given ρ^2 , the feedback bits per user needs to scale as

$$B = (N_t - 1) \log_2 \left(\frac{\delta_0 - 1}{\rho_u^2 P} - \frac{U - 1}{U} \cdot \left(\frac{1}{\rho_u^2} - 1 \right) \right)^{-1}. \quad (24)$$

As $\rho_u^2 \rightarrow 1$, i.e. there is no CSI delay, the condition becomes $B = (N_t - 1) \log_2 \frac{P}{\delta_0 - 1}$, which agrees with the result in [7] with limited feedback only.

2) *Achievable Rate:* For the ZF system with imperfect CSI, the genie-aided upper bound for the ergodic achievable rate⁴ is given by [11]

$$R_{ZF}^{(QD)} \leq \sum_{u=1}^U \mathbb{E}_\gamma \left[\log_2 \left(1 + \gamma_{ZF,u}^{(QD)} \right) \right] = R_{ZF,ub}^{(QD)}. \quad (25)$$

We assume the mobile users can perfectly estimate the noise and interference and feed back it to the transmitter, so the upper bound is chosen as the performance metric, i.e. $R_{ZF}^{(QD)} = R_{ZF,ub}^{(QD)}$, as in [7], [8], [10].

The following lower bound based on the rate loss analysis is used in [7], [11]

$$R_{ZF}^{(QD)} \geq R_{ZF} - \sum_{u=1}^U \log_2 \Delta_{ZF,u}^{(QD)}, \quad (26)$$

where R_{ZF} is the achievable rate with perfect CSIT, given in (9). However, this lower bound is very loose. In the following, we will derive a more accurate approximation for the achievable rate for the ZF system.

To get a good approximation for the achievable rate for the ZF system, we first approximate the instantaneous SINR as

$$\begin{aligned} \gamma_{ZF,u}^{(QD)} &= \frac{\frac{P}{U} |\mathbf{h}_u^*[n] \mathbf{f}_u^{(QD)}[n]|^2}{1 + \frac{P}{U} \sum_{u' \neq u} |(\rho_u \mathbf{h}_u[n-1] + \mathbf{e}_u[n])^* \mathbf{f}_{u'}^{(QD)}[n]|^2} \\ &\approx \frac{\frac{P}{U} |\mathbf{h}_u^*[n] \mathbf{f}_u^{(QD)}[n]|^2}{1 + \frac{P}{U} \left(\sum_{u' \neq u} \rho_u^2 |\mathbf{h}_u^*[n-1] \mathbf{f}_{u'}^{(QD)}[n]|^2 + \sum_{u' \neq u} |\mathbf{e}_u^*[n] \mathbf{f}_{u'}^{(QD)}[n]|^2 \right)}, \end{aligned} \quad (27)$$

i.e. eliminating the interference terms which have both $\mathbf{h}_u[n-1]$ and $\mathbf{e}_u[n]$ as $\mathbf{e}_u[n]$ is normally very small, so we get two separate interference sums due to delay and quantization, respectively.

For the interference term due to delay, $|\mathbf{e}_u^*[n] \mathbf{f}_{u'}^{(QD)}[n]|^2 \sim \chi_2^2$, as $\mathbf{e}_u[n]$ is independent of $\mathbf{f}_{u'}^{(QD)}[n]$ and $\|\mathbf{f}_{u'}^{(QD)}[n]\|^2 = 1$. For the interference term due to quantization, it was shown in [7] that $|\tilde{\mathbf{h}}_u^*[n-1] \mathbf{f}_{u'}^{(QD)}[n]|^2$ is equivalent to the product of the quantization error $\sin^2 \theta_u$ and an independent $\beta(1, N_t - 2)$ random variable. Therefore, we have

$$|\mathbf{h}_u^*[n-1] \mathbf{f}_{u'}^{(QD)}[n]|^2 = \|\mathbf{h}_u[n-1]\|^2 (\sin^2 \theta_u) \cdot \beta(1, N_t - 2). \quad (28)$$

⁴This upper bound is achievable only when a genie provides users with perfect knowledge of all interference and the transmitter knows perfectly the received SINR at each user.

In [10], with a quantization cell approximation⁵ [38], [39], it was shown that $\|\mathbf{h}_u[n-1]\|^2(\sin^2 \theta_u)$ has a Gamma distribution with parameters $(N_t - 1, \delta)$, where $\delta = 2^{-\frac{B}{N_t-1}}$. As shown in [10] the analysis based on the quantization cell approximation is close to the performance of random vector quantization, so we use this approach to derive the achievable rate.

The following lemma gives the distribution of the interference term due to quantization.

Lemma 1: Based on the quantization cell approximation, the interference term due to quantization in (27), $|\mathbf{h}_u[n-1]\mathbf{f}_{u'}^{(QD)}[n]|^2$, is an exponential random variable with mean δ , i.e. its probability distribution function (pdf) is

$$p(x) = \frac{1}{\delta} e^{-x/\delta}, x \geq 0. \quad (29)$$

Proof: See Appendix D. ■

Remark 3: From this lemma, we see that the residual interference terms due to both delay and quantization are exponential random variables, which means the delay and quantization error have equivalent effects, only with different means. By comparing the means of these two terms, i.e. comparing ϵ_e^2 and $2^{-\frac{B}{N_t-1}}$, we can find the dominant one. In addition, with this result, we can approximate the achievable rate of the ZF limited feedback system, which will be provided later in this section.

Based on the distribution of the interference terms, the approximation for the achievable rate for the MU mode is given in the following theorem.

Theorem 4: The ergodic achievable rate for the u -th user in the MU mode with both delay and channel quantization can be approximated as

$$R_{ZF,u}^{(QD)} \approx \log_2(e) \sum_{i=0}^{M-1} \sum_{j=1}^2 \left[a_i^{(j)} i! \left(\frac{\alpha}{\beta} \right)^{i+1} \cdot I_3 \left(\frac{1}{\alpha}, \frac{\alpha}{\beta \delta_j}, i+1 \right) \right], \quad (30)$$

where $\alpha = \beta = \frac{P}{U}$, $\delta_1 = \rho_u^2 \delta$, $\delta_2 = \epsilon_{e,u}^2$, $M = N_t - 1$, $a_i^{(1)}$ and $a_i^{(2)}$ are given in (44) and (45), and $I_3(\cdot, \cdot, \cdot)$ is given in (38) in Appendix A.

Proof: See Appendix E. ■

The ergodic sum throughput is

$$R_{ZF}^{(QD)} = \sum_{u=1}^U R_{ZF,u}^{(QD)}. \quad (31)$$

⁵The quantization cell approximation is based on the ideal assumption that each quantization cell is a Voronoi region on a spherical cap with the surface area 2^{-B} of the total area of the unit sphere for a B bits codebook. The detail can be found in [10], [38], [39].

As a special case, for a ZF system with delay only, we can get the following approximation for the ergodic achievable rate.

Corollary 2: The ergodic achievable rate for the u -th user in the ZF system with delay is approximated as

$$R_{ZF,u}^{(D)} \approx \log_2(e) \left(\frac{\alpha}{\beta} \right)^{-(M-1)} \cdot I_3 \left(\frac{1}{\alpha}, \frac{\alpha}{\beta}, M-1 \right), \quad (32)$$

where $\alpha = \frac{P}{U}$, $\beta = \frac{c_{e,u}^2 P}{U}$, $M = N_t - 1$, and $I_3(\cdot, \cdot, \cdot)$ is given in (38) in Appendix A.

Proof: Following the same steps in Appendix E with $\delta_1 = 0$. ■

Remark 4: As shown in *Lemma 1*, the effects of delay and channel quantization are equivalent, so the approximation in (32) also applies for the limited feedback system. This is verified by simulation in Fig. 1, which shows that this approximation is very accurate and can be used to analyze the limited feedback system.

C. Mode Switching

We first verify the approximation (30) in Fig. 2, which compares the approximation with simulation results and the lower bound (26), with $B = 10$, $v = 20$ km/hr, $f_c = 2$ GHz, and $T_s = 1$ msec. We see that the lower bound is very loose, while the approximation is accurate especially for $N_t = 2$. In fact, the approximation turns out to be a lower bound. Note that due to the imperfect CSIT, the sum rate reduces with N_t .

In Fig. 3, we compare the BF and ZF systems, with $B = 18$, $f_c = 2$ GHz, $v = 10$ km/hr, and $T_s = 1$ msec. We see that the approximation for the BF system almost matches the simulation exactly. The approximation for the ZF system is accurate at low to medium SNRs, and becomes a lower bound at high SNR, which is approximately 0.7 bps/Hz in total, or 0.175 bps/Hz per user, lower than the simulation. The throughput of the ZF system is limited by the residual inter-user interference at high SNR, where it is lower than the BF system. This motivates to switch between the SU and MU MIMO modes. The approximations (17) and (30) will be used to calculate the mode switching points. There may be two switching points for the system with delay, as the SU mode will be selected at both low and high SNR. These two points can be calculated by providing different initial values to the nonlinear equation solver, such as *fsolve* in MATLAB.

V. NUMERICAL RESULTS

In this section, numerical results are presented. First, the operating regions for different modes are plotted, which show the impact of different parameters, including the normalized Doppler frequency, the codebook size, and the number of transmit antennas. Then the extension of our results for the ZF precoding to the MMSE precoding is demonstrated.

A. Operating Regions

As shown in Section IV-C, finding mode switching points requires solving a nonlinear equation, which does not have a closed-form solution and gives little insight. However, it is easy to evaluate numerically for different parameters, from which insights can be drawn. In this section, with the calculated mode switching points for different parameters, we plot the operating regions for both SU and MU modes. The active mode for the given parameter and the condition to activate each mode can be found from such plots.

In Fig. 4, the operating regions for both SU and MU modes are plotted, for different normalized Doppler frequencies and different number of feedback bits in Fig. 4(a) and Fig. 4(b), respectively, and with $U = N_t = 4$. There are analogies between two plots. Some key observations are as follows:

- (i) For the delay plot Fig. 4(a), comparing the two curves for $B = 16$ and $B = 20$, we see that the smaller the codebook size, the smaller the operating region for the ZF mode. For the ZF mode to be active, $f_d T_s$ needs to be small, specifically we need $f_d T_s < 0.055$ and $f_d T_s < 0.046$ for $B = 20$ and $B = 16$, respectively. These conditions are not easily satisfied in practical systems. For example, with carrier frequency $f_c = 2$ GHz, mobility $v = 20$ km/hr, the Doppler frequency is 37 Hz, and then to satisfy $f_d T_s < 0.055$ the delay should be less than 1.5 msec.
- (ii) For the codebook size plot Fig. 4(b), comparing the two curves with $v = 10$ km/hr and $v = 20$ km/hr, as $f_d T_s$ increases (v increases), the ZF operating region shrinks. For the ZF mode to be active, we should have $B \geq 12$ and $B \geq 14$ for $v = 10$ km/hr and $v = 20$ km/hr, respectively, which means a large codebook size. Note that for BF we only need a small codebook size to get the near-optimal performance [5].
- (iii) For a given $f_d T_s$ and B , the SU mode will be active at both low and high SNRs, which is due to its array gain and the robustness to imperfect CSIT, respectively.

The operating regions for different N_t are shown in Fig. 5. We see that as N_t increases, the operating region for the MU mode shrinks. Specifically, we need $B > 12$ for $N_t = 4$, $B > 19$ for $N_t = 6$, and $B > 26$ for $N_t = 8$ to get the MU mode activated. Note that the minimum required feedback bits per user for the MU mode grow approximately linearly with N_t .

B. ZF vs. MMSE Precoding

It is shown in [31] that the regularized ZF precoding, denoted as *MMSE precoding* in this paper, can significantly increase the throughput at low SNR. In this section, we show that our results on mode switching with ZF precoding can also be applied to MMSE precoding.

Denote $\hat{\mathbf{H}}[n] = [\hat{\mathbf{h}}_1[n], \hat{\mathbf{h}}_2[n], \dots, \hat{\mathbf{h}}_U[n]]^*$. Then the MMSE precoding vectors are chosen to be the normalized columns of the matrix [31]

$$\hat{\mathbf{H}}^*[n] \left(\hat{\mathbf{H}}[n] \hat{\mathbf{H}}^*[n] + \frac{U}{P} \mathbf{I} \right)^{-1}. \quad (33)$$

From this, we see that the MMSE precoders converge to ZF precoders at high SNR. Therefore, our derivations for the ZF system also apply to the MMSE system at high SNR.

In Fig. 6, we compare the performance of ZF and MMSE precoding systems with delay⁶. We see that the MMSE precoding outperforms ZF at low to medium SNRs, and converges to ZF at high SNR while converges to BF at low SNR. In addition, it has the same rate ceiling as the ZF system, and crosses the BF curve roughly at the same point, after which we need to switch to the SU mode. Based on this, we can use the second predicted mode switching point (the one at higher SNR) of the ZF system for the MMSE system. We compare the simulation results and calculation results by (19) and (32) for the mode switching points in Table II. For the ZF system, it is the second switching point; for the MMSE system, it is the only switching point. We see that the switching points for MMSE and ZF systems are very close, and the calculated ones are roughly 2.5 ~ 3 dB lower.

VI. CONCLUSIONS

In this paper, we compare the SU and MU MIMO transmissions in the broadcast channel with delayed and quantized CSIT, where the amount of delay and the number of feedback bits per

⁶This can also be done in the system with both delay and quantization, which is more time-consuming. As shown in *Lemma 1*, the effects of delay and quantization are equivalent, so the conclusion will be the same.

user are fixed. The throughput of MU-MIMO saturates at high SNR due to residual inter-user interference, for which a SU/MU mode switching algorithm is proposed. We derive accurate closed-form approximations for the ergodic rates for both SU and MU modes, which are then used to calculate the mode switching points. It is shown that the MU mode is only possible to be active in the medium SNR regime, with a small normalized Doppler frequency and a large codebook size.

For future work, the MU-MIMO mode studied in this paper is designed with zero-forcing criterion, which is shown to be sensitive to CSI imperfections, so robust precoding design is needed and the impact of the imperfect CSIT on non-linear precoding should be investigated. As power control is an effective way to combat interference, it is interesting to consider the efficient power control algorithm rather than equal power allocation to improve the performance, especially in the heterogeneous scenario. It is also of practical importance to investigate possible approaches to improve the quality of the available CSIT with a fixed codebook size, e.g. through channel prediction.

APPENDIX

A. Useful Results for Rate Analysis

In this Appendix, we present some useful results that are used for rate analysis in this paper. The following lemma will be used frequently in the derivation of the achievable rate.

Lemma 2: For a random variable x with probability distribution function (pdf) $f_X(x)$ and cumulative distribution function (cdf) $F_X(x)$, we have

$$\mathbb{E}_X [\ln(1 + X)] = \int_0^\infty \frac{1 - F_X(x)}{1 + x} dx. \quad (34)$$

Proof: The proof follows the integration by parts.

$$\begin{aligned} \mathbb{E}_X [\ln(1 + X)] &= \int_0^\infty \ln(1 + x) f_X(x) dx \\ &= - \int_0^\infty \ln(1 + x) [1 - F_X(x)]' dx \\ &\stackrel{(a)}{=} \int_0^\infty \frac{1 - F_X(x)}{1 + x} dx, \end{aligned} \quad (35)$$

where g' is the derivative of the function g , and step (a) follows the integration by parts. ■

The following lemma provides some useful integrals for rate analysis, which can be derived from the results in [40].

Lemma 3:

$$I_1(a, b, m) = \int_0^\infty \frac{x^m e^{-ax}}{x+b} dx = \sum_{k=1}^m (k-1)! (-b)^{m-k} a^{-k} - (-1)^{m-1} b^m e^{ab} E_1(ab) \quad (36)$$

$$\begin{aligned} I_2(a, b, m) &= \int_0^\infty \frac{e^{-ax}}{(x+b)^m} dx \\ &= \begin{cases} e^{ab} E_1(ab) & m = 1 \\ \sum_{k=1}^{m-1} \frac{(k-1)!}{(m-1)!} \frac{(-a)^{m-k-1}}{b^k} + \frac{(-a)^{m-1}}{(m-1)!} e^{ab} E_1(ab) & m \geq 2 \end{cases} \end{aligned} \quad (37)$$

$$\begin{aligned} I_3(a, b, m) &= \int_0^\infty \frac{e^{-ax}}{(x+b)^m (x+1)} dx \\ &= \sum_{i=1}^m (-1)^{i-1} (1-b)^{-i} \cdot I_2(a, b, m-i+1) + (b-1)^{-m} \cdot I_2(a, 1, 1), \end{aligned} \quad (38)$$

where $E_1(x)$ is the exponential-integral function of the first order.

B. Proof of Theorem 1

The average SNR is

$$\begin{aligned} \overline{\text{SNR}}_{BF}^{(QD)} &= \mathbb{E} \left[P \left| \mathbf{h}^*[n] \mathbf{f}^{(QD)}[n] \right|^2 \right] \\ &= P \mathbb{E} \left[\left| (\rho \mathbf{h}[n-1] + \mathbf{e}[n])^* \hat{\mathbf{h}}[n-1] \right|^2 \right] \\ &\stackrel{(a)}{=} P |\rho \mathbf{h}^*[n-1] \hat{\mathbf{h}}[n-1]|^2 + P |\mathbf{e}^*[n] \hat{\mathbf{h}}[n-1]|^2 \\ &\stackrel{(b)}{\leq} P N_t \rho^2 \left(1 - 2^{-\frac{B}{N_t-1}} \right) + P \mathbb{E} \left[|\hat{\mathbf{h}}^*[n-1] \cdot [\mathbf{e}[n] \mathbf{e}^*[n]] \cdot \hat{\mathbf{h}}[n-1]| \right] \\ &\stackrel{(c)}{=} P N_t \rho^2 \left(1 - 2^{-\frac{B}{N_t-1}} \right) + P \epsilon_e^2, \end{aligned}$$

As $\mathbf{e}[n]$ is independent of $\mathbf{h}[n-1]$, it is also independent of $\hat{\mathbf{h}}[n-1]$, which gives (a). Step (b) follows (11). Step (c) is from the fact $\mathbf{e}[n] \sim \mathcal{CN}(\mathbf{0}, \epsilon_e^2 \mathbf{I}_{N_t})$ and $|\hat{\mathbf{h}}[n-1]|^2 = 1$.

C. Proof of Theorem 2

Denote $y_1 = \|\mathbf{h}[n-1]\|^2$ and $y_2 = \frac{1}{\epsilon_e^2} |\mathbf{e}^*[n] \tilde{\mathbf{h}}[n-1]|^2$, then $y_1 \sim \chi_{2N_t}^2$, $y_2 \sim \chi_2^2$, and they are independent. The received SNR can be written as $x = \eta_1 y_1 + \eta_2 y_2$, where $\eta_1 = P \rho^2$ and

$\eta_2 = P\epsilon_e^2$. The cdf of x is given as [41]

$$F_X(x) = 1 - \left(\frac{\eta_2}{\eta_2 - \eta_1} \right)^{N_t} e^{-x/\eta_2} + e^{-x/\eta_1} \left(\frac{\eta_1}{\eta_2 - \eta_1} \right) \cdot \sum_{i=0}^{N_t-1} \sum_{l=0}^i \frac{1}{(i-l)!} \left(\frac{\eta_2}{\eta_2 - \eta_1} \right)^{N_t-1-i} \left(\frac{x}{\eta_1} \right)^{i-l}. \quad (39)$$

Denote $a_0 = \frac{\eta_2}{\eta_2 - \eta_1}$ and following *Lemma 2* we have

$$\begin{aligned} & \mathbb{E}_X [\ln(1+X)] \\ &= \int_0^\infty \frac{1 - F_X(x)}{1+x} dx \\ &= a_0^{N_t} \int_0^\infty \frac{e^{x/\eta_2}}{1+x} dx - (1 - a_0) \sum_{i=0}^{N_t-1} \sum_{l=0}^i \frac{a_0^{N_t-1-i}}{(i-l)!} \left(\frac{1}{\eta_1} \right)^{i-l} \int_0^\infty \frac{x^{i-l} e^{-x/\eta_1}}{1+x} dx \\ &= a_0^{N_t} I_2(1/\eta_2, 1, 1) - (1 - a_0) \sum_{i=0}^{N_t-1} \sum_{l=0}^i \frac{a_0^{N_t-1-i}}{(i-l)!} \left(\frac{1}{\eta_1} \right)^{i-l} I_1(1/\eta_1, 1, i-l). \end{aligned} \quad (40)$$

where $I_1(\cdot, \cdot, \cdot)$ and $I_2(\cdot, \cdot, \cdot)$ are given in (36) and (37), respectively.

D. Proof of Lemma 1

Let $x = \|\mathbf{h}_u[n-D]\|^2 \sin^2 \theta \sim \Gamma(M-1, \delta)$, $y \sim \beta(1, M-2)$, and x is independent of y . Then the interference term due to quantization is $z = xy$. The cdf of z is

$$\begin{aligned} P_Z(z) &= P(xy \leq z) \\ &= \int_0^\infty F_{Y|X} \left(\frac{z}{x} \right) f_X(x) dx \\ &= \int_0^z f_X(x) dx + \int_z^\infty \left(1 - \left(1 - \frac{z}{x} \right)^{M-2} \right) f_X(x) dx \\ &= \int_0^\infty f_X(x) dx - \int_z^\infty \left(1 - \frac{z}{x} \right)^{M-2} x^{M-2} \frac{e^{-x/\delta}}{(M-2)! \delta^{M-1}} dx \\ &= 1 - e^{-z/\delta} \int_z^\infty (x-z)^{M-2} \frac{e^{-(x-z)/\delta}}{(M-2)! \delta^{M-1}} dx \\ &\stackrel{(a)}{=} 1 - e^{-z/\delta}, \end{aligned} \quad (41)$$

where step (a) follows the equality $\int_0^\infty y^M e^{-\alpha y} dy = M! \alpha^{-(M+1)}$.

E. Proof of Theorem 4

Assuming each interference term in (27) is independent of each other and independent of the signal power term, denote $\sum_{u' \neq u} \rho_u^2 |\mathbf{h}_u^*[n-1] \mathbf{f}_{u'}^{(QD)}[n]|^2 = \rho_u^2 \delta y_1$ and $\sum_{u' \neq u} |\mathbf{e}_u^*[n] \mathbf{f}_{u'}^{(QD)}[n]|^2 = \epsilon_{e,u}^2 y_2$, then from *Lemma 1* we have $y_1 \sim \chi_{2(N_t-1)}^2$, and $y_2 \sim \chi_{2(N_t-1)}^2$ as $\mathbf{e}_u[n]$ is complex Gaussian with variance $\epsilon_{e,u}^2$ and independent of the normalized vector $\mathbf{f}_{u'}^{(QD)}[n]$. In addition, the signal power $|\mathbf{h}_u^*[n] \mathbf{f}_u^{(QD)}[n]|^2 \sim \chi_2^2$. Then the received SINR for the u -th user is approximated as

$$\gamma_{ZF,u}^{(QD)} \approx \frac{\alpha z}{1 + \beta(\delta_1 y_1 + \delta_2 y_2)} \triangleq x, \quad (42)$$

where $\alpha = \beta = \frac{P}{U}$, $\delta_1 = \rho_u^2 \delta$, $\delta_2 = \epsilon_{e,u}^2$, $y_1 \sim \chi_{2M}^2$, $y_2 \sim \chi_{2M}^2$, $M = N_t - 1$, $z \sim \chi_2^2$, and y_1, y_2, z are independent of each other.

Let $y = \delta_1 y_1 + \delta_2 y_2$, then the pdf of y , which is the sum of two independent chi-square random variables, is given as [41]

$$\begin{aligned} p_Y(y) &= e^{-y/\delta_1} \sum_{i=0}^{M-1} a_i^{(1)} y^i + e^{-y/\delta_2} \sum_{i=0}^{M-1} a_i^{(2)} y^i \\ &= \sum_{j=1}^2 \sum_{i=0}^{M-1} e^{-y/\delta_j} a_i^{(j)} y^i, \end{aligned} \quad (43)$$

where

$$a_i^{(1)} = \frac{1}{\delta_1^{i+1} (M-1)!} \left(\frac{\delta_1}{\delta_1 - \delta_2} \right)^M \frac{(2(M-1) - i)!}{i! (M-1-i)!} \left(\frac{\delta_2}{\delta_2 - \delta_1} \right)^{M-1-i} \quad (44)$$

$$a_i^{(2)} = \frac{1}{\delta_2^{i+1} (M-1)!} \left(\frac{\delta_2}{\delta_2 - \delta_1} \right)^M \frac{(2(M-1) - i)!}{i! (M-1-i)!} \left(\frac{\delta_1}{\delta_1 - \delta_2} \right)^{M-1-i}. \quad (45)$$

The cdf of x is

$$\begin{aligned} F_X(x) &= P\left(\frac{\alpha z}{1 + \beta y} \leq x\right) \\ &= \int_0^\infty F_{Z|Y}\left(\frac{x}{\alpha}(1 + \beta y)\right) p_Y(y) dy \\ &= \int_0^\infty (1 - e^{-\frac{x}{\alpha}(1 + \beta y)}) p_Y(y) dy \\ &= 1 - e^{-x/\alpha} \int_0^\infty e^{-\beta x y / \alpha} p_Y(y) dy \\ &= 1 - e^{-x/\alpha} \int_0^\infty \left\{ \sum_{j=1}^2 \sum_{i=0}^{M-1} \exp\left[-\left(\frac{\beta}{\alpha}x + \frac{1}{\delta_j}\right)y\right] a_i^{(j)} y^i \right\} dy \end{aligned}$$

$$\stackrel{(a)}{=} 1 - e^{-x/\alpha} \sum_{j=1}^2 \sum_{i=0}^{M-1} \left[\frac{a_i^{(j)} i!}{\left(\frac{\beta}{\alpha} x + \frac{1}{\delta_j}\right)^{i+1}} \right], \quad (46)$$

where step (a) follows the equality $\int_0^\infty y^M e^{-\alpha y} = M! \alpha^{-(M+1)}$.

Then the ergodic achievable rate for the u -th user is approximated as

$$\begin{aligned} R_{ZF,u}^{(QD)} &= \mathbb{E}_\gamma \left[\log_2 \left(1 + \gamma_{ZF,u}^{(QD)} \right) \right] \\ &\approx \log_2(e) \mathbb{E}_X [\ln(1 + X)] \\ &\stackrel{(a)}{=} \log_2(e) \int_0^\infty \frac{1 - F_X(x)}{x + 1} dx \\ &= \log_2(e) \int_0^\infty \sum_{i=0}^{M-1} \sum_{j=1}^2 \left[a_i^{(j)} i! \left(\frac{\alpha}{\beta} \right) \frac{e^{-x/\alpha}}{\left(x + \frac{\alpha}{\beta \delta_j}\right)^{i+1} (x + 1)} \right] dx \\ &\stackrel{(b)}{=} \log_2(e) \sum_{i=0}^{M-1} \sum_{j=1}^2 \left[a_i^{(j)} i! \left(\frac{\alpha}{\beta} \right)^{i+1} I_3 \left(\frac{1}{\alpha}, \frac{\alpha}{\beta \delta_j}, i + 1 \right) \right], \end{aligned} \quad (47)$$

where step (a) follows from *Lemma 2*, step (b) follows the expression of $I_3(\cdot, \cdot, \cdot)$ in (38).

REFERENCES

- [1] I. E. Telatar, "Capacity of mulit-antenna Gaussian channels," *Europ. Trans. Telecommun.*, vol. 10, pp. 585–595, Nov. 1999.
- [2] A. Goldsmith, S. A. Jafar, N. Jindal, and S. Vishwanath, "Capacity limits of MIMO channels," *IEEE J. Select. Areas Commun.*, vol. 51, no. 6, pp. 684–702, Jun. 2003.
- [3] D. Gesbert, M. Kountouris, R. W. Heath, Jr., C. B. Chae, and T. Salzer, "Shifting the MIMO paradigm: From single user to multiuser communications," *IEEE Signal Processing Magazine*, vol. 24, no. 5, pp. 36–46, Sept. 2007.
- [4] B. Hassibi and M. Sharif, "Fundamental limits in MIMO broadcast channels," *IEEE J. Select. Areas Commun.*, vol. 25, no. 7, pp. 1333–1344, Sept. 2007.
- [5] D. J. Love, R. W. Heath, Jr., W. Santipach, and M. Honig, "What is the value of limited feedback for MIMO channels?" *IEEE Commun. Mag.*, vol. 42, no. 10, pp. 54–59, Oct. 2004.
- [6] D. J. Love, R. W. Heath, Jr., V. K. N. Lau, D. Gesbert, B. D. Rao, and M. Andrews, "An overview of limited feedback in wireless communication systems," *IEEE J. Select. Areas Commun.*, vol. 26, no. 8, pp. 1341–1365, Oct. 2008.
- [7] N. Jindal, "MIMO broadcast channels with finite rate feedback," *IEEE Trans. Inform. Theory*, vol. 52, no. 11, pp. 5045–5059, Nov. 2006.
- [8] P. Ding, D. J. Love, and M. D. Zoltowski, "Multiple antenna broadcast channels with partial and limited feedback," *IEEE Trans. Signal Processing*, vol. 55, no. 7, pp. 3417–3428, Jul. 2007.
- [9] N. Ravindran and N. Jindal, "Limited feedback-based block diagonalization for the MIMO broadcast channel," *IEEE J. Select. Areas Commun.*, vol. 26, no. 8, pp. 1473–1482, Oct. 2008.
- [10] T. Yoo, N. Jindal, and A. Goldsmith, "Multi-antenna downlink channels with limited feedback and user selection," *IEEE J. Select. Areas Commun.*, vol. 25, no. 7, pp. 1478–1491, Sept. 2007.

- [11] G. Caire, N. Jindal, M. Kobayashi, and N. Ravindran, "Multiuser MIMO downlink made practical: Achievable rates with simple channel state estimation and feedback schemes," *Submitted to IEEE Trans. Information Theory*, 2007, available online at <http://arxiv.org/pdf/0711.2642>.
- [12] G. Caire, N. Jindal, and S. Shamai, "On the required accuracy of transmitter channel state information in multiple antenna broadcast channels," in *Proc. of the IEEE Asilomar Conf. on Signals, Systems, and Computers*, Pacific Grove, CA, Nov. 2007, pp. 289–291.
- [13] N. Ravindran, N. Jindal, and H. C. Huang, "Beamforming with finite rate feedback for LOS MIMO downlink channels," in *Proc. IEEE Globecom*, Washington, DC, Nov. 2007, pp. 4200–4204.
- [14] S. Haykin, *Adaptive Filter Theory*, 3rd ed. Englewood Cliffs, NJ: Prentice-Hall, 1996.
- [15] R. H. Clarke, "A statistical theory of mobile radio reception," *Bell System Tech. J.*, vol. 47, pp. 957–1000, 1968.
- [16] E. N. Onggosanusi, A. Gatherer, A. G. Dabak, and S. Hosur, "Performance analysis of closed-loop transmit diversity in the presence of feedback delay," *IEEE Trans. Commun.*, vol. 49, no. 9, pp. 1618–1630, Sept. 2001.
- [17] H. T. Nguyen, J. B. Anderson, and G. F. Pedersen, "Capacity and performance of MIMO systems under the impact of feedback delay," in *Proc. of the IEEE Int. Symp. on Personal Indoor and Mobile Radio Comm.*, Barcelona, Spain, Sept. 2004, pp. 53–57.
- [18] H. Poor, *An introduction to signal detection and estimation*. New York, NY, USA: Springer-Verlag New York, Inc., 1994.
- [19] G. Caire, N. Jindal, M. Kobayashi, and N. Ravindran, "Quantized vs. analog feedback for the MIMO broadcast channel: A comparison between zero-forcing based achievable rates," in *Proc. IEEE Int. Symp. Information Theory*, Nice, France, Jun. 2007, pp. 2046–2050.
- [20] M. Kobayashi and G. Caire, "Joint beamforming and scheduling for a multi-antenna downlink with imperfect transmitter channel knowledge," *IEEE J. Select. Areas Commun.*, vol. 25, no. 7, pp. 1468–1477, Sept. 2007.
- [21] W. Santipach and M. Honig, "Asymptotic capacity of beamforming with limited feedback," in *Proc. IEEE Int. Symp. Information Theory*, Chicago, IL, Jun./Jul. 2004, p. 290.
- [22] C. K. Au-Yeung and D. J. Love, "On the performance of random vector quantization limited feedback beamforming in a MISO system," *IEEE Trans. Wireless Commun.*, vol. 6, no. 2, pp. 458–462, Feb. 2007.
- [23] M. Alouini and A. Goldsmith, "Capacity of Rayleigh fading channels under different adaptive transmission and diversity-combining techniques," *IEEE Trans. Veh. Technol.*, vol. 48, no. 4, pp. 1165–1181, Jul. 1999.
- [24] M. Costa, "Writing on dirty paper," *IEEE Trans. Inform. Theory*, vol. 39, no. 3, pp. 439–441, May 1983.
- [25] G. Caire and S. Shamai (Shitz), "On the achievable throughput of a multiantenna Gaussian broadcast channel," *IEEE Trans. Inform. Theory*, vol. 49, no. 7, pp. 1691–1706, Jul. 2003.
- [26] W. Yu and J. Cioffi, "The sum capacity of a Gaussian vector broadcast channel," *IEEE Trans. Inform. Theory*, vol. 50, no. 9, pp. 1875–1892, Sep. 2004.
- [27] S. Vishwanath, N. Jindal, and A. Goldsmith, "Duality, achievable rates, and sum-rate capacity of MIMO broadcast channels," *IEEE Trans. Inform. Theory*, vol. 49, no. 10, pp. 2658–2668, Oct. 2003.
- [28] P. Viswanath and D. N. C. Tse, "Sum capacity of the vector Gaussian broadcast channel and uplink-downlink duality," *IEEE Trans. Inform. Theory*, vol. 49, no. 8, pp. 1912–1921, Aug. 2003.
- [29] H. Weingarten, Y. Steinberg, and S. Shamai, "The capacity region of the Gaussian multiple-input multiple-output broadcast channel," *IEEE Trans. Inform. Theory*, vol. 52, no. 9, pp. 3936–3964, Sept. 2006.
- [30] N. Jindal, "A high SNR analysis of MIMO broadcast channels," in *Proc. IEEE Int. Symp. Information Theory*, Adelaide, Australia, Sept. 2005, pp. 2310–2314.

- [31] C. Peel, B. Hochwald, and A. Swindlehurst, "Vector-perturbation technique for near-capacity multiantenna multiuser communication-Part I: Channel inversion and regularization," *IEEE Trans. Commun.*, vol. 53, no. 1, pp. 195–202, Jan. 2005.
- [32] V. K. N. Lau and M. Jiang, "Performance analysis of multiuser downlink space-time scheduling for TDD systems with imperfect CSIT," *IEEE Trans. Veh. Technol.*, vol. 55, no. 1, pp. 296–305, Jan. 2006.
- [33] T. Wu and V. K. N. Lau, "Robust rate, power and precoder adaptation for slow fading MIMO channels with noisy limited feedback," *IEEE Trans. Wireless Commun.*, vol. 7, no. 6, pp. 2360–2367, Jun. 2008.
- [34] A. Vakili, M. Sharif, and B. Hassibi, "The effect of channel estimation error on the throughput of broadcast channels," in *Proc. of the IEEE Int. Conf. on Acoustics, Speech, and Signal Proc.*, Toulouse, France, May 2006, pp. IV 29–32.
- [35] A. Vakili and B. Hassibi, "On the throughput of broadcast channels with imperfect CSI," in *Proc. of IEEE SPAWC*, Cannes, France, Jul. 2006, pp. 1–5.
- [36] A. Vakili, A. F. Dana, and B. Hassibi, "On the throughput of opportunistic beamforming with imperfect CSI," in *Proc. of ACM IWCMC*, Honolulu, HI, Aug. 2007, pp. 19–23.
- [37] M. Kountouris, R. de Francisco, D. Gesbert, D. T. M. Slock, and T. Salzer, "Efficient metrics for scheduling in MIMO broadcast channels with limited feedback," in *Proc. of the IEEE Int. Conf. on Acoustics, Speech, and Signal Proc.*, Honolulu, USA, Apr. 2007, pp. 109–112.
- [38] K. Muekkavilli, A. Sabharwal, E. Erkip, and B. Aazhang, "On beamforming with finite rate feedback in multiple-antenna systems," *IEEE Trans. Inform. Theory*, vol. 49, no. 10, pp. 2562–2579, Oct. 2003.
- [39] S. Zhou, Z. Wang, and G. B. Giannakis, "Quantifying the power loss when transmit beamforming relies on finite rate feedback," *IEEE Trans. Wireless Commun.*, vol. 4, no. 7, pp. 1948–1957, Jul. 2005.
- [40] I. S. Gradshteyn and I. M. Ryzhik, *Table of Integrals, Series, and Products*, 5th ed. San Diego, CA: Academic, 1994.
- [41] M. K. Simon, *Probability Distributions Involving Gaussian Random Variables: A Handbook for Engineers and Scientists*. Springer, 2002.

TABLE I
SYSTEM PARAMETERS

Symbol	Description
N_t	number of transmit antennas
U	number of mobile users
B	number of feedback bits
L	quantization codebook size, $L = 2^B$
P	average SNR
n	time index
T_s	the length of each symbol
f_d	the Doppler frequency

TABLE II
MODE SWITCHING POINTS

	$f_d T_s = 0.03$	$f_d T_s = 0.04$	$f_d T_s = 0.05$
MMSE (Simulation)	44.2 dB	35.7 dB	29.5 dB
ZF (Simulation)	44.2 dB	35.4 dB	28.6 dB
ZF (Calculation)	41.6 dB	32.9 dB	26.1 dB

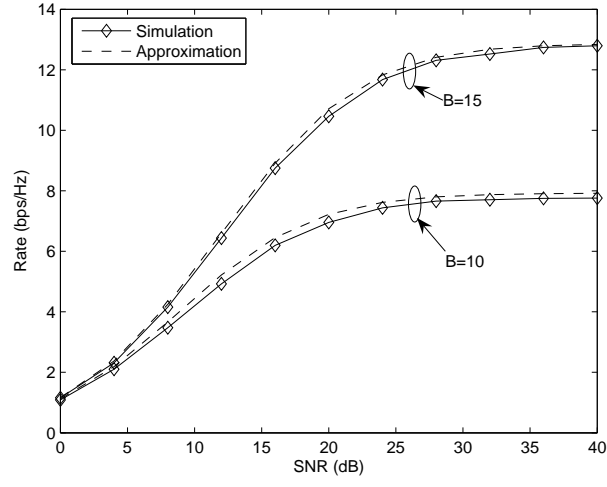


Fig. 1. Approximations and simulations for the ZF system with limited feedback, $N_t = U = 4$.

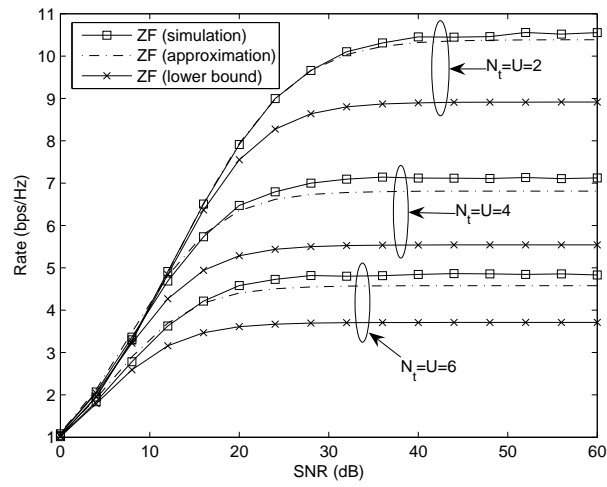


Fig. 2. Comparison of approximation in (30), the lower bound in (26), and the simulation results for the ZF system with both delay and channel quantization. $B = 10$, $f_c = 2$ GHz, $v = 20$ km/hr, and $T_s = 1$ msec.

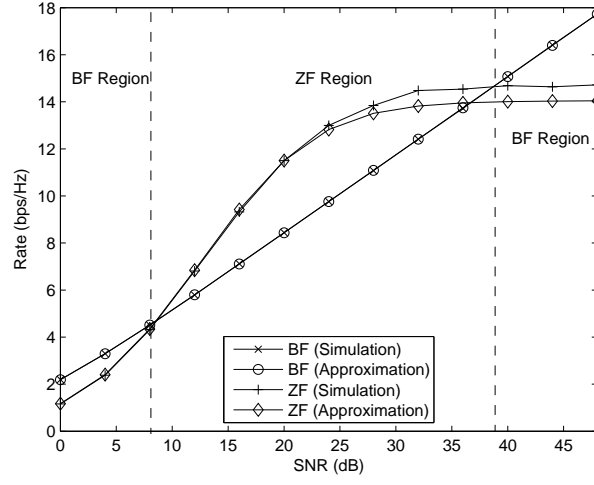
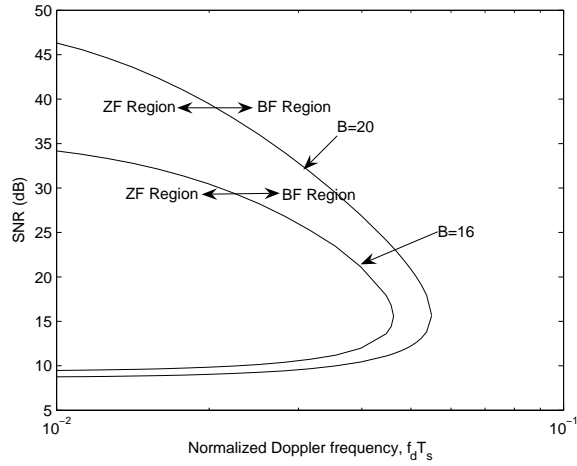
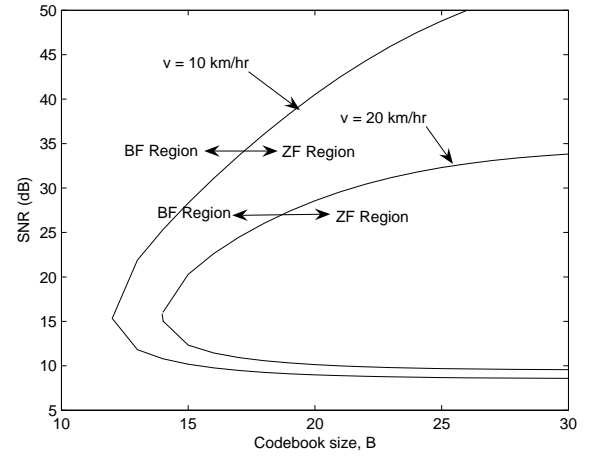


Fig. 3. Mode switching between BF and ZF modes with both CSI delay and channel quantization, $B = 18$, $N_t = 4$, $f_c = 2$ GHz, $T_s = 1$ msec, $v = 10$ km/hr.



(a) Different $f_d T_s$.



(b) Different B , $f_c = 2$ GHz, $T_s = 1$ msec.

Fig. 4. Operating regions for BF and ZF with both CSI delay and quantization, $N_t = 4$.

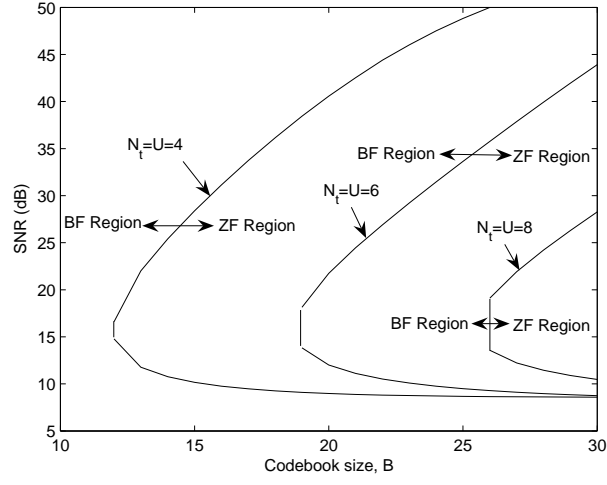


Fig. 5. Operating regions for BF and ZF with different N_t , $f_c = 2$ GHz, $v = 10$ km/hr, $T_s = 1$ msec.

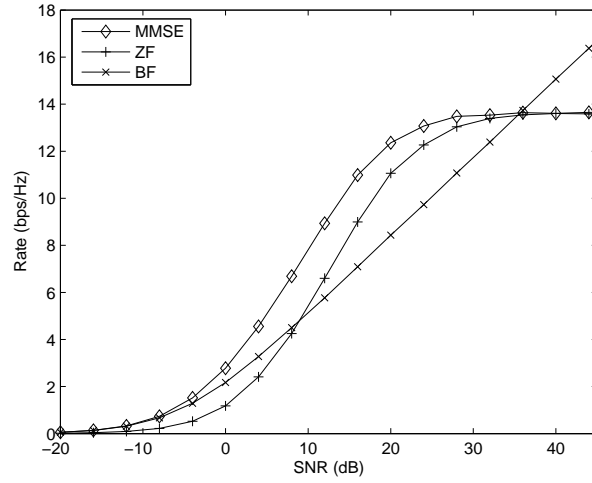


Fig. 6. Simulation results for BF, ZF and MMSE systems with delay, $N_t = U = 4$, $f_d T_s = 0.04$.